

Article

Research on Multiple Load Short-Term Forecasting Model of Integrated Energy Distribution System Based on Mogrifier-Quantum Weighted MELSTM

Peng Song and Zhisheng Zhang *

School of Electrical Engineering, Qingdao University, Qingdao 266071, China; 2021020640@qdu.edu.cn

* Correspondence: slnzzs@126.com; Tel.: +86-131-8899-8256

Abstract: Accurate and efficient short-term forecasting of multiple loads is of great significance to the operation control and scheduling of integrated energy distribution systems. In order to improve the effect of load forecasting, a mogrifier-quantum weighted memory enhancement long short-term memory (Mogrifier-QWMELSTM) neural network forecasting model is proposed. Compared with the conventional LSTM neural network model, the model proposed in this paper has three improvements in model structure and model composition. First, the mogrifier is added to make the data fully interact with each other. This addition can help enhance the correlation between the front and rear data and improve generalization, which is the main disadvantage of LSTM neural network. Second, the memory enhancement mechanism is added on the forget gate to realize the extraction and recovery of forgotten information. The addition can help improve the gradient transmission ability in the learning process of the neural network, make the neural network remain sensitive to distant data information, and enhance the memory ability. Third, the model is composed of quantum weighted neurons. Compared with conventional neurons, quantum weighted neurons have significant advantages in nonlinear data processing and parallel computing, which help to improve the accuracy of load forecasting. The simulation results show that the weighted mean accuracy of the proposed model can reach more than 97.5% in summer and winter. Moreover, the proposed model has good forecasting effect on seven typical days in winter, which shows that the model has good stability.



Citation: Song, P.; Zhang, Z. Research on Multiple Load Short-Term Forecasting Model of Integrated Energy Distribution System Based on Mogrifier-Quantum Weighted MELSTM. *Energies* **2023**, *16*, 3697. <https://doi.org/10.3390/en16093697>

Academic Editor: Javier Contreras

Received: 29 March 2023

Revised: 21 April 2023

Accepted: 24 April 2023

Published: 25 April 2023



Copyright: © 2023 by the authors. Licensee MDPI, Basel, Switzerland. This article is an open access article distributed under the terms and conditions of the Creative Commons Attribution (CC BY) license (<https://creativecommons.org/licenses/by/4.0/>).

Keywords: integrated energy distribution system; multiple load forecasting; mogrifier; memory enhancement mechanism; quantum weighted neuron

1. Introduction

In recent years, the problem of environmental pollution and ecological destruction has become increasingly serious. It is imperative to vigorously develop new energy and promote the transformation and upgrading of the energy industry [1]. The integrated energy distribution system (IEDS) takes typical energy supply networks such as distribution network, gas distribution network and regional thermal network as the backbone grid. Taking energy hubs as typical energy coupling links, it is an integrated system of production, supply and marketing realized after coordinating and optimizing the production, distribution, conversion and consumption of multiple energy sources. It has the characteristics of a complex energy structure, diverse energy consumption characteristics, intensive energy interaction and strong coupling of physical information. IEDS plays an important role in the transformation and upgrading of the energy industry, which is of great significance for improving the environmental quality and energy utilization rate [2]. The construction of IEDS helps to solve a series of challenges and problems faced by the development of the energy industry.

Accurate and efficient short-term forecasting of multiple loads is of great significance to the operation control and scheduling of IEDS [3]. Firstly, according to the results of

multiple load forecasting, various energy sources are rationally allocated to improve the energy utilization efficiency and the economy of IEDS operation [4]. Secondly, according to the results of multiple load forecasting, the demand side analysis and the response plan are made more reasonably, which can help improve the reliability of IEDS operation [5]. Finally, based on the results of multiple load forecasting, the maintenance department sets maintenance time and makes a maintenance plan reasonably to avoid the peak period of energy consumption and reduce the influence on the user side of the system [6]. In recent years, various types of neural networks have been widely used in multiple load short-term forecasting and achieved good forecasting results [7]. Luo et al. [8] constructed a load forecasting model by combining a convolution neural network with support vector machine. Li et al. [9] applied wavelet neural network to short-term load forecasting. They used an improved particle swarm optimization algorithm to optimize the wavelet neural network. Zhu et al. [10] comprehensively considered the autocorrelation of various loads in time series and the cross-correlation in various frequency bands, and constructed a wavelet packet decomposition-recurrent neural network forecasting model. Zhang et al. [11] proposed a short-term load forecasting method based on a deep belief network and multi-task regression, which considers energy conversion and consumption modes. Zhou et al. [12] proposed a multiple load short-term forecasting method based on user hierarchical clustering and deep belief network. They clustered user groups into different clusters which can help improve forecasting performance.

Long short-term memory (LSTM) neural network is an improved variant of recurrent neural network (RNN). Compared with RNN, LSTM neural network redesigns the memory cell on the basis of maintaining the basic structure and sets up three control gates, namely forget gate, input gate and output gate. The three control gates are used to select the correction parameters of the error function of memory feedback which descends with the gradient, and to optimize the weight of the self-loop, so as to keep the dynamic change of the weight [13]. LSTM neural network has good nonlinear data fitting ability, so it is applied to multiple load forecasting of IEDS, which is a nonlinear time series forecasting problem. Tian et al. [14] applied a conventional LSTM neural network to multiple load short-term forecasting. Sun et al. [15] established a shared layer of multi-task learning through LSTM neural network to realize multiple load forecasting. However, the conventional LSTM neural network has poor stability and its ability to extract input features from high-dimensional and long-order data is insufficient. Its generalization ability and forecasting accuracy need to be improved. Tian et al. [16] added an attention mechanism and dropout layer to the LSTM neural network to build forecasting model. These two improvements can help to reduce training time, enhance stability and improve the forecasting effect. Zheng et al. [17] combined Copula theory with deep bidirectional LSTM neural network to build a forecasting model. The advantage of bidirectional learning is helpful to improve the accuracy of load forecasting. However, Tian et al. [16] and Zheng et al. [17] did not verify the generalization ability and stability of the proposed models. In recent years, many new research results have been put forward about the structural improvement of LSTM neural network. Melis et al. [18] constructed a mogrifier LSTM neural network to improve the generalization ability of the neural network. Wu et al. [19] added the memory enhancement mechanism to LSTM neural network to realize the extraction and recovery of forgotten information. This addition can help improve the gradient conduction ability and memory ability of the neural network.

Combining quantum computing theory with neural networks is considered to be an effective way to improve the performance of neural networks, and has become a hot topic in neural network research [20]. Compared with conventional neural networks, quantum neural networks have more advantages in parallel computing and have stronger nonlinear data processing capabilities. Li et al. [21] applied a quantum neural network combined with depth self-coding network to snow-covered flashover voltage prediction. Wang et al. [22] constructed a gas outburst risk grade prediction model based on an optimized quantum gated-node neural network. In recent years, the quantum weighted neural network, which

is a common form of quantum neural networks, has been applied in the field of multiple load short-term forecasting [23].

Based on the existing research results, aiming at the defects and deficiencies of LSTM neural network model, a forecasting model based on mogrifier-quantum weighted memory enhancement long short-term memory neural network is proposed in this paper. The model is improved from two aspects: model structure and model composition. In terms of model structure, the mogrifier and memory enhancement mechanism are added to improve the generalization ability and the input feature extraction ability of high-dimensional and long-order data, which are disadvantages of the LSTM neural network. In terms of model composition, the model is composed of quantum weighted neurons. The advantages of quantum weighted neurons in nonlinear data processing and parallel computing are fully utilized to improve the forecasting accuracy and stability. The simulation results show that these three improvements are effective.

The structure of this paper is as follows. Section 2 introduces the theory of the quantum weighted neuron and the model proposed in this paper, including its structure, improvements and operation process. Section 3 includes the selection of input characteristic variables, the setting of model parameters, the forecasting effect of the proposed model and the comparison with other models. Section 4 shows the research conclusions of this paper.

2. Multiple Load Short-Term Forecasting Model of Based on Mogrifier-Quantum Weighted MELSTM

2.1. Quantum Weighted Neuron

In quantum computing system, the expression of a quantum state is as follows [24]:

$$|\phi\rangle = a|0\rangle + b|1\rangle = [a, b]^T \quad (1)$$

where $|\cdot\rangle$ is the Dirac symbol, $|0\rangle = [1, 0]^T$, $|1\rangle = [0, 1]^T$, a and b are a pair of complex numbers, which represent the probability amplitude of quantum state, $|a|^2 + |b|^2 = 1$.

In quantum weighted neurons, transmitter transfer from cell to cell is simulated by four steps, which are weighting, aggregation, activation and excitation [25]. Weighting is the simulation of the binding strength between synapses in nerve cells. Aggregation is the simulation of stimuli collected by dendrites. Activation is the simulation of the change of membrane potential and the interaction between membrane potential and current activity value. Excitation is the simulation of the nonlinear characteristics of neurons such as inhibition, fatigue and threshold. The structure of quantum weighted neurons is shown in Figure 1. Weight values and activity values are expressed by quantum states respectively, and activation is realized by the inner product operator.

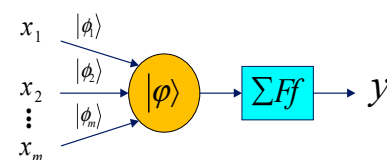


Figure 1. Structure diagram of quantum weighted neurons.

In Figure 1, $|\phi_m\rangle$, $|\phi\rangle$, Σ , F and f represent the quantum state of weight value, the quantum state of activity value, the aggregation operator, the activation function and the excitation function, respectively, $|\phi_m\rangle = [\cos \alpha_m, \sin \alpha_m]^T$, $|\phi\rangle = [\cos \beta, \sin \beta]^T$, α_m is the phase of $|\phi_m\rangle$, and β is the phase of $|\phi\rangle$.

The input is $x = [x_1, x_2, \dots, x_m]^T$, the output is y , the input and output expression of a quantum weighted neuron is as follows:

$$\begin{aligned}
 y &= f(F(x^T|\phi), |\varphi\rangle) \\
 &= f\left(\sum_{i=1}^m x_i \langle \phi_i | \varphi \rangle\right) \\
 &= f\left(\sum_{i=1}^m x_i \cos(\alpha_i - \beta)\right)
 \end{aligned}
 \tag{2}$$

where $|\phi\rangle = [|\phi_1\rangle, |\phi_2\rangle, \dots, |\phi_m\rangle]^T$ denotes the quantum state vector of weight value, $|\phi_i\rangle = [\cos \alpha_i, \sin \alpha_i]^T$ and $|\varphi\rangle = [\cos \beta, \sin \beta]^T$ denote the quantum state of weight value and the quantum state of activity value, respectively, α_i is the phase of $|\phi_i\rangle$, and β is the phase of $|\varphi\rangle$. Updating α_i and β can update $|\phi_i\rangle$ and $|\varphi\rangle$.

2.2. Mogrifier-QWMELSTM Neural Network Forecasting Model

The structure of Mogrifier-QWMELSTM neural network forecasting model constructed in this paper is shown in Figure 2. Compared with the conventional LSTM neural network, the basic structures such as the forget gate and input gate remain unchanged. The model is improved in two aspects: model structure and model composition. In terms of model structure, there are two improvements. First, the mogrifier is added to make x_t and h_{t-1} complete interaction and update before making relevant calculations. This addition can help enhance the correlation between the front and rear data, and improve generalization ability of neural network. Second, the memory enhancement mechanism is added on the forget gate to realize the extraction and recovery of forgotten information. This addition can help improve the gradient transmission ability in the learning process of the neural network, make the neural network remain sensitive to distant data information, and enhance the memory ability. In terms of model composition, the model is composed of quantum weighted neurons. Compared with conventional neurons, they have significant advantages in nonlinear data processing and parallel computing, which is helpful to enhance the generalization ability and nonlinear approximation ability of neural network.

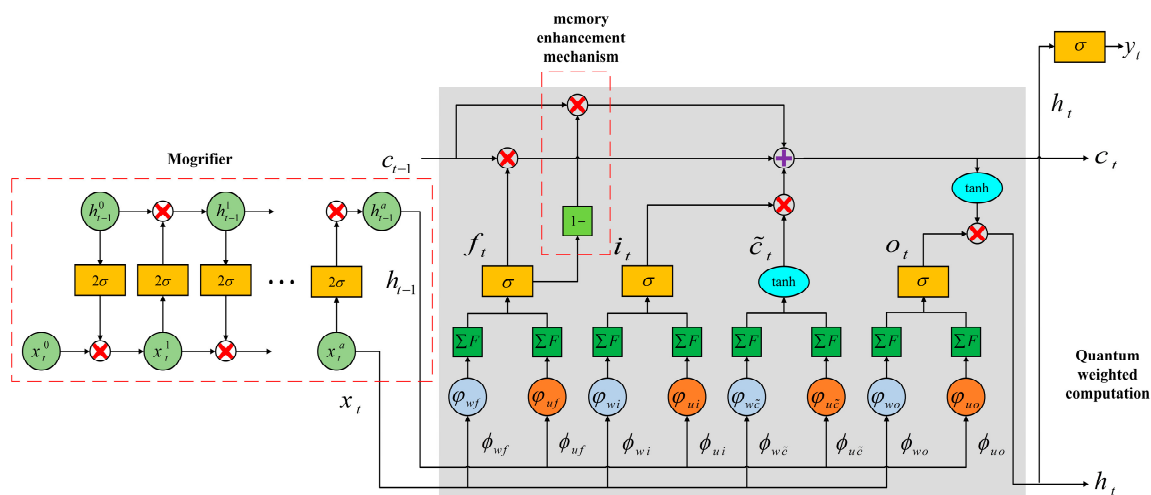


Figure 2. Structure diagram of Mogrifier-QWMELSTM neural network.

The input of the model at the current moment x_t^0 and the output of the hidden layer at the moment $t - 1$ h_{t-1}^0 are interacted and updated by weighting and excitation.

$$x_t = x_t^a = 2\sigma(Q \cdot h_{t-1}^{a-1}) \times x_t^{a-1} \tag{3}$$

$$h_{t-1} = h_{t-1}^a = 2\sigma(R \cdot x_t^{a-1}) \times h_{t-1}^{a-1} \tag{4}$$

In the formula, Q is the weight matrix connected with h_t , R is the weight matrix connected with x_t , σ is the sigmoid function, and a is the number of updates of the mogrifer.

After interaction and updating, x_t and h_{t-1} are weighted, aggregated and activated, and then excited by sigmoid function and tanh function to obtain f_t , i_t , \tilde{c}_t , and o_t .

$$\begin{aligned} f_t^j &= \sigma(U_f \cdot h_{t-1} + W_f \cdot x_t + b_f)^j \\ &= \sigma(F(h_{t-1}^T | \phi_{uf}(j)), |(\varphi_{uf})_j\rangle) + F(x_t^T | \phi_{wf}(j)), |(\varphi_{wf})_j\rangle) + b_f^j \\ &= \sigma(\sum_{l=1}^s h_{t-1}^l \cos((\alpha_{uf})_{lj} - (\beta_{uf})_j) + \sum_{n=1}^p x_t^n \cos((\alpha_{wf})_{nj} - (\beta_{wf})_j) + b_f^j) \end{aligned} \quad (5)$$

$$\begin{aligned} i_t^j &= \sigma(U_i \cdot h_{t-1} + W_i \cdot x_t + b_i)^j \\ &= \sigma(F(h_{t-1}^T | \phi_{ui}(j)), |(\varphi_{ui})_j\rangle) + F(x_t^T | \phi_{wi}(j)), |(\varphi_{wi})_j\rangle) + b_i^j \\ &= \sigma(\sum_{l=1}^s h_{t-1}^l \cos((\alpha_{ui})_{lj} - (\beta_{ui})_j) + \sum_{n=1}^p x_t^n \cos((\alpha_{wi})_{nj} - (\beta_{wi})_j) + b_i^j) \end{aligned} \quad (6)$$

$$\begin{aligned} \tilde{c}_t^j &= \tanh(U_{\tilde{c}} \cdot h_{t-1} + W_{\tilde{c}} \cdot x_t + b_{\tilde{c}})^j \\ &= \tanh(F(h_{t-1}^T | \phi_{u\tilde{c}}(j)), |(\varphi_{u\tilde{c}})_j\rangle) + F(x_t^T | \phi_{w\tilde{c}}(j)), |(\varphi_{w\tilde{c}})_j\rangle) + b_{\tilde{c}}^j \\ &= \tanh(\sum_{l=1}^s h_{t-1}^l \cos((\alpha_{u\tilde{c}})_{lj} - (\beta_{u\tilde{c}})_j) + \sum_{n=1}^p x_t^n \cos((\alpha_{w\tilde{c}})_{nj} - (\beta_{w\tilde{c}})_j) + b_{\tilde{c}}^j) \end{aligned} \quad (7)$$

$$\begin{aligned} o_t^j &= \sigma(U_o \cdot h_{t-1} + W_o \cdot x_t + b_o)^j \\ &= \sigma(F(h_{t-1}^T | \phi_{uo}(j)), |(\varphi_{uo})_j\rangle) + F(x_t^T | \phi_{wo}(j)), |(\varphi_{wo})_j\rangle) + b_o^j \\ &= \sigma(\sum_{l=1}^s h_{t-1}^l \cos((\alpha_{uo})_{lj} - (\beta_{uo})_j) + \sum_{n=1}^p x_t^n \cos((\alpha_{wo})_{nj} - (\beta_{wo})_j) + b_o^j) \end{aligned} \quad (8)$$

In the formula, U_f , U_i , $U_{\tilde{c}}$, and U_o are the weight matrices connected with h_{t-1} , W_f , W_i , $W_{\tilde{c}}$, and W_o are the weight matrices connected with x_t , b_f , b_i , $b_{\tilde{c}}$, and b_o are bias vectors, ϕ_{uf} and φ_{uf} denote the quantum state of weight value and the quantum state of activity value constituting U_f , respectively, α_{uf} is the phase of ϕ_{uf} , and β_{uf} is the phase of φ_{uf} . Similarly, ϕ_{wf} , ϕ_{ui} , ϕ_{wi} , $\phi_{u\tilde{c}}$, $\phi_{w\tilde{c}}$, ϕ_{uo} , and ϕ_{wo} denote the quantum states of weight value constituting corresponding weight matrices, φ_{wf} , φ_{ui} , φ_{wi} , $\varphi_{u\tilde{c}}$, $\varphi_{w\tilde{c}}$, φ_{uo} , and φ_{wo} denote the quantum states of activity value constituting corresponding weight matrices and α_{wf} , α_{ui} , α_{wi} , $\alpha_{u\tilde{c}}$, $\alpha_{w\tilde{c}}$, α_{uo} , α_{wo} , β_{wf} , β_{ui} , β_{wi} , $\beta_{u\tilde{c}}$, $\beta_{w\tilde{c}}$, β_{uo} , and β_{wo} are the phases of corresponding quantum states. p is the number of units in the input layer, and s is the number of units in the hidden layer. $n = 1, 2, \dots, p$, $j = 1, 2, \dots, s$ and $l = 1, 2, \dots, s$. σ is the sigmoid excitation function and \tanh is the tanh excitation function.

The memory cell state at the current moment c_t is calculated from the memory cell state at the moment $t - 1$ c_{t-1} , the forgetting information $c_{t-1(f)}$, f_t and \tilde{c}_t . h_t is calculated from c_t excited by the tanh excitation function and o_t .

$$c_{t-1(f)}^j = (1 - f_t^j) \times c_{t-1}^j \quad (9)$$

$$c_t^j = f_t^j \times c_{t-1}^j + W c_{t-1(f)}^j + i_t^j \times \tilde{c}_t^j \quad (10)$$

$$h_t^j = o_t^j \times \tanh(c_t^j) \quad (11)$$

In the formula, W is the selection ratio of forgetting information.

The output of the hidden layer h_t is weighted and excited by sigmoid excitation function to obtain the output of the model y_t .

$$y_t^k = \sigma(W_y h_t)^k \quad (12)$$

In the formula, W_y is the weight matrix connected with h_t , q is the number of units in the output layer, $k = 1, 2, \dots, q$.

3. Example Simulation

3.1. Example Setting and Parameter Setting

In this paper, DeST simulation software [26–28] is used to obtain the data of the integrated energy distribution system in northern China for one year. The IEDS is of commercial type and runs from 8:00 to 21:00. The obtained data include electrical load, cooling load, heating load and weather influencing factors. The electrical load and cooling load are mainly considered in summer, and the electrical load and heating load are mainly considered in winter. Temperature is the key factor affecting the electrical load, cooling load and heating load in IEDS. Solar radiation is closely related to the temperature and has a direct impact on the temperature change. Moisture content is related to human body temperature, which has an indirect effect on the changes of three loads. Therefore, temperature, moisture content and solar radiation are selected as three weather-influencing factors to participate in the correlation analysis. In this paper, the grey relational analysis method is used for correlation analysis. The results are shown in Tables 1 and 2. EL, HL and CL represent electrical load, heating load and cooling load, respectively. T, M and R represent temperature, moisture content and solar radiation, respectively.

Table 1. Correlation between loads and influencing factors in summer.

Load Type	Correlation Degree				
	EL	CL	T	M	R
EL	1.00	0.87	0.63	0.59	0.75
CL	0.87	1.00	0.65	0.63	0.78

Table 2. Correlation between loads and influencing factors in winter.

Load Type	Correlation Degree				
	EL	HL	T	M	R
EL	1.00	0.76	0.63	0.64	0.76
HL	0.75	1.00	0.64	0.68	0.78

From the results, there is a strong coupling among cooling load, heating load and electrical load. The three weather factors of temperature, moisture content and solar radiation are closely related to the electrical load, cooling load and heating load of IEDS, which have an important impact on them.

Characteristic quantities of the input are shown in Figure 3, divided into weather data and historical data. The weather data include three kinds of weather factors at the moments $t - 1$, t and $t + 1$ on the forecast day. The historical data include the historical loads at the moment $t - 1$ on the forecast day and at the moments $t - 1$, t , $t + 1$ on the day before the forecast day. All input data need to be normalized.

The number of units in the hidden layer is 95, the number of updates of the mogrifer is 3, and the selection ratio of forgotten information is set to 0.2. The model is optimized by Adam algorithm. The initial learning rate is set to 0.01 and the number of iterations is set to 6000. The hardware configuration of this experiment is Intel Core i7-12700H CPU. The memory is 16 G. The software platforms adopted are Python language and Pytorch framework.

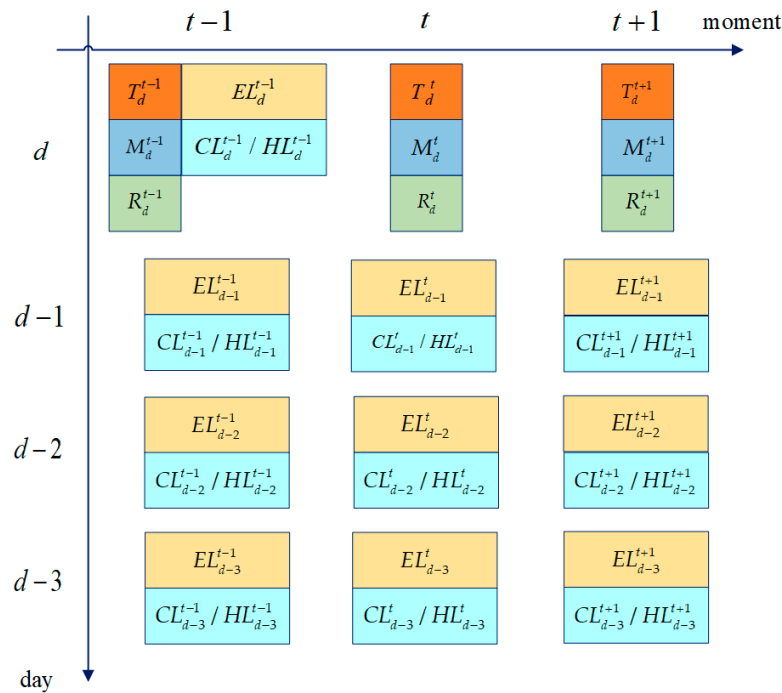


Figure 3. Characteristic quantities of the input.

3.2. Evaluating Indicator

The mean absolute percentage error (MAPE) and the weighted mean accuracy (WMA) are used as evaluation indexes to evaluate the performance and forecasting effect of the forecasting model [29]. The calculation formulas are as follows:

$$MAPE = \frac{1}{n} \sum_{i=1}^n \left| \frac{a_i - b_i}{a_i} \right| \times 100\% \tag{13}$$

$$MA = 1 - MAPE \tag{14}$$

$$WMA = \alpha_1 MA_1 + \alpha_2 MA_2 + \dots + \alpha_k MA_k \tag{15}$$

where a_i and b_i are the actual value and forecasting value of load at the moment i , respectively, n is the number of load forecasting points, α_k is the weight of load of class k and MA_k is the mean accuracy of load of class k .

Considering the difference of importance of different energy sources in IEDS [30], the weights of electrical load and cooling load are set to 0.6 and 0.4, respectively, in the joint forecasting of electric load and cooling load in summer. The weights given to the joint forecasting of electrical load and heating load in winter are the same as above.

3.3. Load Forecasting Process

The multiple load forecasting process based on Mogrifler-QWMELSTM is shown in Figure 4.

3.4. Comparison of Forecasting Effects

In order to verify the effectiveness of the model proposed in this paper, typical days are selected for forecasting and analysis. Considering the difference of load between working days and rest days, a typical working day and a typical rest day are selected in summer and winter, respectively. Conventional LSTM neural network forecasting model (Model 1), mogrifler-LSTM neural network forecasting model (Model 2), memory enhancement LSTM neural network forecasting model (Model 3) and mogrifler-memory enhancement LSTM

neural network forecasting model (Model 4) are selected as comparison models. The above four models are simulated together with the model proposed in this paper (Model 5). The structure of Model 4 is the same as that of Model 5, and the neurons of Model 4 are conventional neurons.

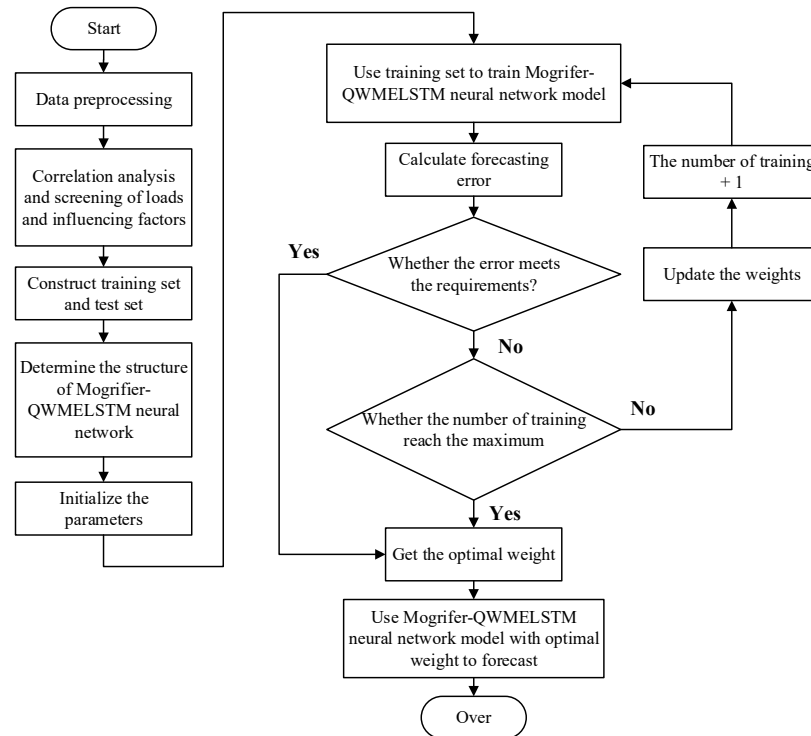


Figure 4. Flow chart of load forecasting.

Figures 5 and 6 show the forecasting curves of electrical load and cooling load of five forecasting models on working day and rest day in summer. It can be seen that the fitting degree between the load forecasting curve of Model 5 and the true value curve is better than that of the other four forecasting models. The forecasting errors of the five forecasting models are large near the peak of electrical load curve and cooling load curve. The reason for this is that the changeable weather conditions in summer lead to great fluctuations at the peak of load curve, which increases the difficulty of load forecasting.

The forecasting effect of the five models are shown in Figure 7, Tables 3 and 4. In the load forecasting of four typical days, the WMA of Model 2 is increased by 0.748%, 0.712%, 0.714% and 0.648%, respectively, compared with Model 1, which shows that the mogrifier is added to make the data fully interact with each other, enhance the correlation between the front and rear data and help to improve the model performance. The WMA of Model 3 is increased by 0.562%, 0.49%, 0.432% and 0.438%, respectively, compared with Model 1, which shows that the memory enhancement mechanism is added to improve the gradient transmission ability in the learning process of the neural network, enhance the memory ability and improve the accuracy of load forecasting. The WMA of Model 4 reached more than 97% on four typical days, and the forecasting effect of Model 4 is better than that of Model 2 and Model 3, indicating that the mogrifier and memory enhancement mechanism can work together to further improve the forecasting accuracy. The WMA of Model 5 is increased by 0.722%, 0.842%, 0.626% and 0.638%, respectively, compared with Model 4, which shows that modeling with quantum weighted neurons can improve the learning ability of neural network, and improve the forecasting effect.

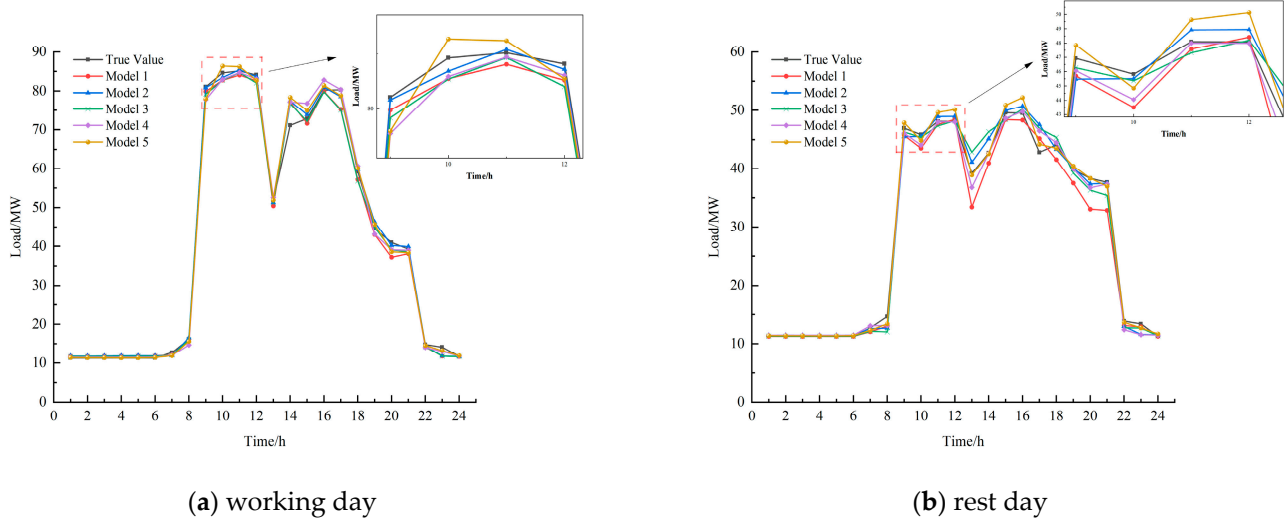


Figure 5. Comparison of electrical load forecasting curves of five models in summer. (a) Electrical load forecasting curves of five models on working day in summer; (b) Electrical load forecasting curves of five models on rest day in summer.

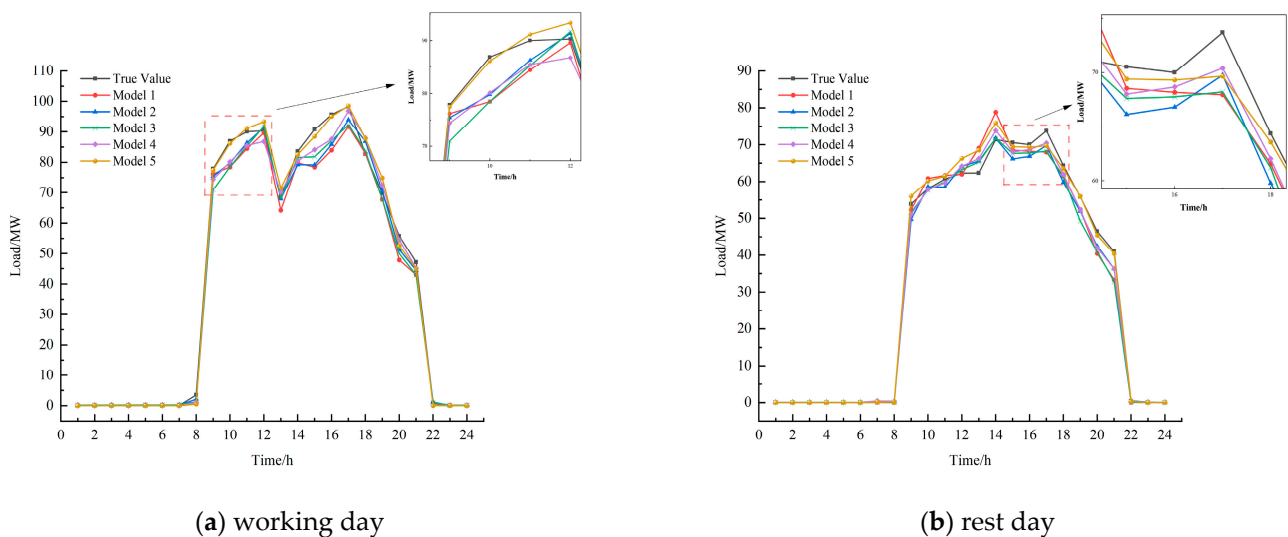


Figure 6. Comparison of cooling load forecasting curves of five models in summer. (a) Cooling load forecasting curves of five models on working day in summer; (b) Cooling load forecasting curves of five models on rest day in summer.

In order to verify the stability of the model proposed in this paper, seven typical days in winter are selected for forecasting. The results are shown in Table 5. The WMA of the proposed model in these seven days is over 97.5%.

To sum up, adding mogrifier and memory enhancement mechanism to conventional LSTM neural network and modeling with quantum weighted neurons can effectively improve the performance of the neural network and improve the forecasting effect of the model. The model proposed in this paper has a good forecasting effect in both summer and winter, and the stability of the model is also very good.

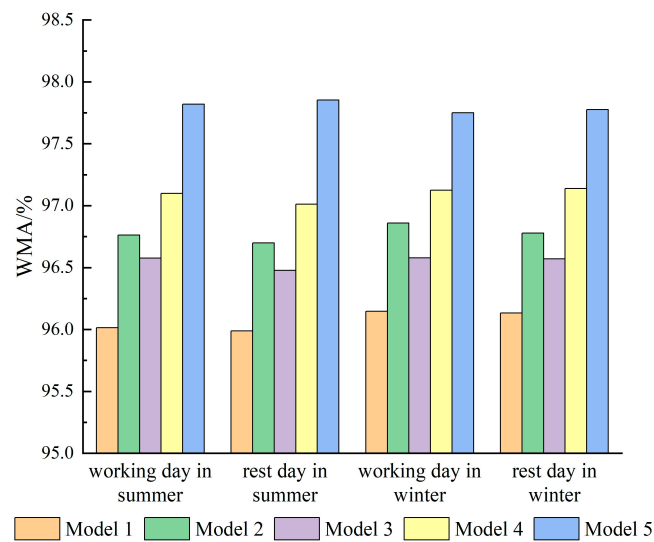


Figure 7. Comparison of weighted mean accuracy of five models.

Table 3. Comparison of forecasting effect of five models in summer.

		Working Day		Rest Day	
		Electrical Load	Cooling Load	Electrical Load	Cooling Load
MAPE/%	Model 1	4.19	3.68	4.28	3.61
	Model 2	3.45	2.92	3.52	2.97
	Model 3	3.58	3.19	3.75	3.18
	Model 4	3.13	2.56	3.28	2.55
	Model 5	2.54	1.64	2.33	1.87
WMA/%	Model 1	96.014		95.988	
	Model 2	96.762		96.700	
	Model 3	96.576		96.478	
	Model 4	97.098		97.012	
	Model 5	97.820		97.854	

Table 4. Comparison of forecasting effect of five models in winter.

		Working Day		Rest Day	
		Electrical Load	Heating Load	Electrical Load	Heating Load
MAPE/%	Model 1	3.77	3.98	3.82	3.94
	Model 2	3.04	3.29	3.17	3.30
	Model 3	3.33	3.56	3.37	3.52
	Model 4	2.76	3.05	2.77	3.00
	Model 5	2.01	2.61	2.04	2.50
WMA/%	Model 1	96.146		96.132	
	Model 2	96.860		96.778	
	Model 3	96.578		96.570	
	Model 4	97.124		97.138	
	Model 5	97.750		97.776	

Table 5. Forecasting effect of the model in seven typical days.

	MAPE/%		WMA/%
	Electrical Load	Heating Load	
Day 1	2.37	2.38	97.626
Day 2	2.19	2.26	97.782
Day 3	2.06	2.27	97.856
Day 4	2.22	2.29	97.752
Day 5	2.01	2.61	97.750
Day 6	2.04	2.50	97.776
Day 7	2.37	2.47	97.590

4. Conclusions

IEDS plays an important role in the transformation and upgrading of the energy industry, which is of great significance to improve the environmental quality and energy utilization rate. Accurate and efficient short-term forecasting of multiple loads is of great significance to the operation control and scheduling of IEDS and can provide a reference for the dispatching department and maintenance department. In this paper, a multiple load short-term forecasting model of IEDS based on Mogrifier-QWMELSTM is proposed. In order to verify the forecasting effect of the model, a large number of simulation experiments are carried out. The simulation results show that the proposed model has good forecasting accuracy and stability. Compared with the conventional LSTM neural network forecasting model, the model has made the following improvements in model structure and model composition:

- (1) The mogrifier is added to make the data fully interact with each other. This addition can help enhance the correlation between the front and rear data and improve the model's generalization ability, which is the disadvantage of LSTM neural network.
- (2) The memory enhancement mechanism is added on the forget gate to realize the extraction and recovery of forgotten information. This addition can help improve the gradient transmission ability in the learning process of the neural network, make the neural network remain sensitive to distant data information and enhance the model's memory ability.
- (3) The model is composed of quantum weighted neurons. Compared with conventional neurons, quantum weighted neurons have significant advantages in nonlinear data processing and parallel computing, which can help improve the accuracy of load forecasting.

In the future, the structure of IEDS will be more complex and energy access will be more diverse. Therefore, the requirement of forecasting accuracy will become higher. In the following research, the applicability of the forecasting model will be considered emphatically, and the forecasting model will be applied to various types of IEDS load forecasting for verification and analysis. At the same time, the model structure will continue to be optimized to improve the load forecasting accuracy.

Author Contributions: Writing—original draft preparation, P.S.; writing—review and editing, Z.Z. All authors have read and agreed to the published version of the manuscript.

Funding: This research was funded by National Natural Science Foundation of China, grant number 52077108.

Data Availability Statement: Not applicable.

Acknowledgments: The work was supported by National Natural Science Foundation of China (52077108).

Conflicts of Interest: The authors declare no conflict of interest.

References

1. Hasan, M.M.; Wu, C. Estimating energy-related CO₂ emission growth in Bangladesh: The LMDI decomposition method approach. *Energy Strategy Rev.* **2020**, *32*, 100565. [[CrossRef](#)]
2. Tan, Z.; De, G.; Li, M.; Lin, H.; Yang, S.; Huang, L.; Tan, Q. Combined electricity-heat-cooling-gas load forecasting model for integrated energy system based on multi-task learning and least square support vector machine. *J. Clean. Prod.* **2019**, *248*, 119252. [[CrossRef](#)]
3. Wang, X.; Wang, S.; Zhao, Q.; Wang, S.; Fu, L. A multi-energy load prediction model based on deep multi-task learning and ensemble approach for regional integrated energy systems. *Int. J. Electr. Power Energy Syst.* **2021**, *126*, 106583.
4. Wu, C.; Yao, J.; Xue, G.; Wang, J.; Wu, Y.; He, K. Load forecasting of integrated energy system based on MMOE multi-task learning and LSTM. *Electr. Power Autom. Eq.* **2022**, *42*, 33–39.
5. Talaat, M.; Farahat, M.A.; Mansour, N.; Hatata, A.Y. Load forecasting based on grasshopper optimization and a multilayer feed-forward neural network using regressive approach. *Energy* **2020**, *196*, 117087. [[CrossRef](#)]
6. Zhang, X. Research on Multi-Load Short-Term Forecasting of Regional Integrated Energy System. Master's Thesis, North China Electric Power University, Beijing, China, 2022.
7. Zhu, J.; Dong, H.; Li, S.; Chen, Z.; Luo, T. Review of Data-driven Load Forecasting for Integrated Energy System. *Proc. CSEE* **2021**, *41*, 7905–7924.
8. Luo, F.; Zhang, X.; Yang, X.; Yao, Z.; Zhu, L.; Qian, M. Load analysis and prediction of integrated energy distribution system based on deep learning. *High Volt. Eng.* **2021**, *47*, 23–32.
9. Li, S.; Qi, J.; Bai, X.; Ge, L.; Li, T. A short-term load prediction of integrated energy system based on IPSO-WNN. *Electr. Meas. Instrum.* **2020**, *57*, 103–109.
10. Zhu, L.; Wang, X.; Ma, J.; Chen, Q.; Qi, X. Short-term load forecast of integrated energy system based on wavelet packet decomposition and recurrent neural network. *Electr. Power Constr.* **2020**, *41*, 131–138.
11. Zhang, L.; Shi, J.; Wang, L.; Xu, C. Electricity, Heat, and Gas Load Forecasting Based on Deep Multitask Learning in Industrial-Park Integrated Energy System. *Entropy* **2020**, *22*, 1355. [[CrossRef](#)]
12. Zhou, B.; Meng, Y.; Huang, W.; Wang, H.; Deng, L.; Huang, S.; Wei, J. Multi-energy net load forecasting for integrated local energy systems with heterogeneous prosumers. *Int. J. Electr. Power Energy Syst.* **2021**, *126*, 106542. [[CrossRef](#)]
13. Wang, S.; Takyi-Aninakwa, P.; Jin, S.; Yu, C.; Fernandez, C.; Stroe, D. An improved feedforward-long short-term memory modeling method for the whole-life-cycle state of charge prediction of lithium-ion batteries considering current-voltage-temperature variation. *Energy* **2022**, *254*, 124224. [[CrossRef](#)]
14. Tian, H.; Han, A.; Yu, L.; Zhang, Z. Research on multi-load short-term forecasting model of regional integrated energy system based on GRA-LSTM neural network. *Guangdong Electr. Power* **2020**, *33*, 44–51.
15. Sun, Q.; Wang, X.; Zhang, Y.; Zhang, F.; Zhang, P.; Gao, W. Multiple load prediction of integrated energy system based on long short-term memory and multi-task learning. *Autom. Electr. Power Syst.* **2021**, *45*, 63–70.
16. Tian, H.; Zhang, Z.; Yu, D. Research on multi-load short-term forecasting of regional integrated energy system based on improved LSTM. *Proc. CSU-EPSCA* **2021**, *33*, 130–137.
17. Zheng, J.; Zhang, L.; Chen, J.; Wu, G.; Ni, S.; Hu, Z.; Weng, C.; Chen, Z. Multiple-Load Forecasting for Integrated Energy System Based on Copula-DBiLSTM. *Energies* **2021**, *14*, 2188. [[CrossRef](#)]
18. Melis, G.; Kocishy, T.; Blunsom, P. Mogrifier LSTM. In Proceedings of the International Conference on Learning Representations, Addis Ababa, Ethiopia, 30 April 2020.
19. Wu, M.; Hou, L.; Wang, C. Improved Mechanism of Prediction-Oriented Long Short-Term Memory Neural Network. *Comput. Eng. Appl.* **2021**, *57*, 109–115.
20. Ding, L. Research on Quantum Neural Network Model and Its Algorithm. Master's Thesis, Northwest University, Xi'an, China, 2009.
21. Li, Y.; Teng, Y.; Yuan, S.; Leng, O. Study on snow covered insulator flashover characteristics and its improved QNN prediction model. *Power Syst. Technol.* **2018**, *42*, 2725–2732.
22. Wang, Y.; Sun, F.; Fu, H.; Xu, Y. Prediction of Coal and Gas Outburst Based on Optimized Quantum Gated Neural Networks. *Inf. Contrl.* **2020**, *49*, 249–256.
23. Wang, S.; Zhang, Z. Short-Term Multiple Load Forecasting Model of Regional Integrated Energy System Based on QWGRU-MTL. *Energies* **2021**, *14*, 6555. [[CrossRef](#)]
24. Zhu, Y. Research on Quantum Neural Network Model of Structure and Algorithm. Master's Thesis, Northeast University, Shenyang, China, 2012.
25. Xiang, W.; Li, F.; Wang, J.; Tang, B. Quantum Weighted Gated Recurrent Unit Neural Network and Its Application in Performance Degradation Trend Prediction of Rotating Machinery. *Neurocomputing* **2018**, *313*, 85–95. [[CrossRef](#)]
26. Sun, F.; Li, N.; Chen, S.; Xie, Y. Comparison Analysis Between Simulation and Practice Measurement of Energy Consumption Based on DEST-H Software in Urban Residence. *Power Gener. Technol.* **2007**, *118*, 43–46.
27. Dong, X. Research on Multi-Featured Heating Load Prediction Based on LSTM Neural Network. Master's Thesis, North China Electric Power University, Beijing, China, 2022.
28. Zhu, S.; Yu, X. Economic Benefits of Energy-saving Reconstruction of Existing Farm Houses in Tianjin Based on DeST. *J. BEE* **2022**, *50*, 121–125+143.

29. Wang, S.; Ren, P.; Takyi-Aninakwa, P.; Jin, S.; Fernandez, C. A Critical Review of Improved Deep Convolutional Neural Network for Multi-Timescale State Prediction of Lithium-Ion Batteries. *Energies* **2022**, *15*, 5053. [[CrossRef](#)]
30. Shi, J.; Tan, T.; Guo, J.; Liu, Y.; Zhang, J. Multi-task learning based on deep architecture for various types of load forecasting in regional energy system integration. *Power Syst. Technol.* **2018**, *42*, 698–707.

Disclaimer/Publisher’s Note: The statements, opinions and data contained in all publications are solely those of the individual author(s) and contributor(s) and not of MDPI and/or the editor(s). MDPI and/or the editor(s) disclaim responsibility for any injury to people or property resulting from any ideas, methods, instructions or products referred to in the content.